

Low Temperature Copper-Nanorod Bonding for 3D Integration

Pei-I Wang¹, Tansel Karabacak², Jian Yu³, Hui-Feng Li⁴, Gopal G. Pethuraja¹, Sang Hwui Lee¹, Michael Z. Liu¹, J.-Q. Lu¹, and T.-M. Lu¹

¹Center of Integrated Electronics, Rensselaer Polytechnic Institute, Troy, NY, 12180

²Now with Department of Applied Science, University of Arkansas at Little Rock, Little Rock, AR, 72204

³Now with IBM, Fishkill, NY, 12524

⁴Now with Freescale Semiconductor, Austin, TX, 78729

ABSTRACT

Wafer bonding is an emerging technology for fabrication of complex three-dimensional (3D) structures; particularly it enables monolithic wafer-level 3D integration of high performance, multi-function microelectronic systems. For such a 3D integrated circuits, low-temperature wafer bonding is required to be compatible with the back-end-of-the-line processing conditions. Recently our investigation on surface melting characteristics of copper nanorod arrays showed that the threshold of the morphological changes of the nano-rod arrays occurs at a temperature significantly below the copper bulk melting point. With this unique property of the copper nanorod arrays, wafer bonding using copper nanorod arrays as a bonding intermediate layer was investigated at low temperatures (400 °C and lower). 200 mm Wafers, each with a copper nanorod array layer, were bonded at 200 – 400 °C and with a bonding down-force of 10 kN in a vacuum chamber. Bonding results were evaluated by razor blade test, mechanical grinding and polishing, and cross-section imaging using a focus ion beam/scanning electron microscope (FIB/SEM). The FIB/SEM images show that the copper nanorod arrays fused together accompanying by a grain growth at a bonding temperature of as low as 200 °C. A dense copper bonding layer was achieved at 400 °C where copper grains grew throughout the copper structure and the original bonding interface was eliminated. The sintering of such nanostructures depends not only on their feature size, but also significantly influenced by the bonding pressure. These two factors both contribute to the mass transport in the nanostructure, leading to the formation of a dense bonding layer.

INTRODUCTION

Wafer bonding is an emerging and promising technology for the manufacturing of complex three-dimensional (3D) structures. Photolithography, which enables the mass production and batch fabrication of Micro-Electro-Mechanical Systems (MEMS) devices, is subject to the limited manufacturability of 3D structures, resulting in a narrow design space and deterioration in the device performance. In wafer bonding, device wafers are patterned individually to create semi-3D structures by microfabrication and, subsequently, bonded together to form complex 3D structures at the wafer level. Wafer bonding started in MEMS as a process that helped form a part of a device and provided a first-level package.¹ From MEMS, wafer bonding is now advancing microelectronics² and optoelectronics.^{3,4}

The continuing push for smaller and faster electronics has led to tremendous advances in the scale of circuit integration and packaging density. For decades, advances in device scaling

and miniaturization worked in a collaborative manner where decreasing sizes typically improved performance. Today, however, developments in technology have pushed functional integration to such a high level that interconnect and packaging issues represent real barriers to further progress. While significant research effort has been expended on various planar approaches, 3D technology is undoubtedly gaining increasing momentum as a leading contender in the challenge to meet performance, cost, and size demands through this decade and beyond.⁵ Wafer bonding can complement established 3D stacking approaches and makes them more efficient.

Because industry has shifted to copper instead of conventionally used aluminum as the interconnect metal since copper has better conductivity and is less susceptible to electro-migration, copper is being particularly attractive as the bonding media for wafer bonding for 3D interconnect. Copper bonding has been studied extensively.^{6,7} The bonding mechanism in their studies relies on atomic diffusion in solid state upon thermal annealing.

Recently we have reported the investigation of the melting characteristics of copper nanorod arrays grown by an oblique angle deposition technique.⁸ It was observed that surface melting disintegration of the copper nanorod arrays occurred at temperatures significantly lower than its bulk melting point. These results suggested low temperature soldering/bonding applications for the copper nanorod arrays. In this study, wafer bonding by copper nanorod arrays at temperatures of 400 °C or lower is investigated. The morphological changes and microstructures of the wafer bonding were characterized using focus ion beam/scanning electron microscope (FIB/SEM). The melting point depression of such nanostructures owing to size effect and bonding pressure enhanced mass transport is discussed and elucidated.

EXPERIMENT

After RCA cleaning, a thermal oxide was grown to a thickness about 500 nm on <100> 200 mm silicon wafers. A 50 nm thick tantalum film (as adhesion layer) and a 500 nm thick copper film were deposited, in sequence, without breaking the vacuum using a CVC sputter system. The sputtering power for tantalum and copper were 1.65 kW and 2.3 kW, respectively. The base pressure was in the range of 10^{-7} Torr. The argon pressure during the sputtering was 5 mTorr. This process was followed by oblique angle deposition of a 500 nm thick copper nanorod layer in an electron-beam evaporator. The wafers were attached to a sample holder to maintain an angle of 85° between the surface normal of the substrate and the surface normal of the evaporation source during the deposition. The base pressure during the deposition was in the range of 10^{-7} Torr. The copper rods were measured to be about 50 nm in diameter and 760 nm in length.

Wafer bonding was carried out in the EV501 bonder (EV Group). After N₂ purge, the chamber was evacuated to a base pressure of 2×10^{-4} mbar and subsequently ramped in a rate of 32 °C/min. Once the bonder temperature reached the set point (400°C/300°C/200°C), a uniform down force of 10 kN (equivalent to 0.32 MPa across 200 mm diameter wafers) was applied and maintained for 1 hour for bonding process. The bonded wafers were unloaded after the chamber cooled down. The mechanical integrity of the bonded wafer pairs was evaluated qualitatively, using both a razor blade insertion test and a three-step backside thinning evaluation (grinding/polishing/wet-etching). The bonded wafer pairs were cleaved into halves for razor blade insertion test and backside thinning evaluation, respectively. Both of the wafer pairs that were bonded at 300 °C and 400 °C passed the razer blade insertion, while the wafer pairs bonded at 200 °C failed the test due to the partially bonded interface, which will be discussed in next

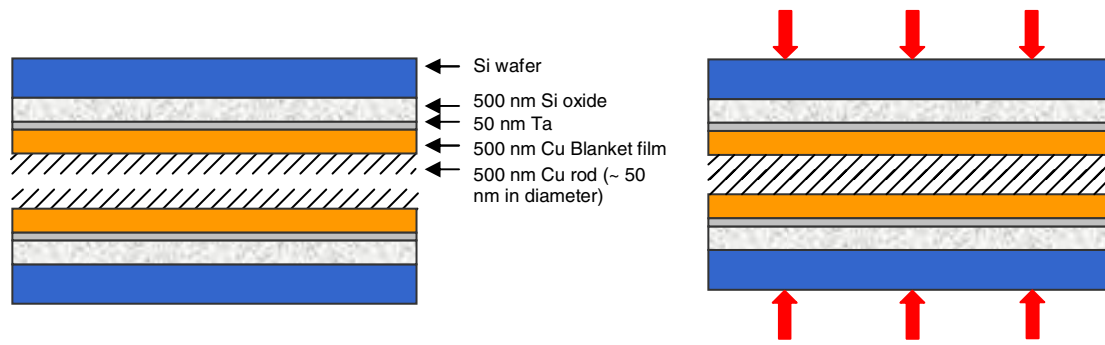


Figure 1 Schematic illustration of the copper nanorod bonding.

section.

One backside of the bonded silicon wafer pair was ground and polished. The remaining silicon layer were then removed using TetraMethylAmoniumHydroxide (TMAH) diluted with distilled water (2:1) at 90 °C for 1-2 hours. This recipe provides an etching rate of about 1 $\mu\text{m}/\text{min}$ for silicon. TMAH etches silicon selectively over silicon oxide.

Cross-sectional microscopy was performed on the backside thinned wafer pairs in a dual beam system Zeiss Ultra 1540 XBeam, combining a focus ion beam (FIB) and a scanning electron microscopy (SEM) at 54 ° angle. By working at a coincidence of ion and electron beam, the system permits FIB milling and in situ SEM on a sample simultaneously. FIB milling was performed at 30 kV acceleration voltages and SEM was performed at 5 kV acceleration voltages.

RESULTS AND DISCUSSION

Figure 1 illustrates a schematic of our wafer bonding approach, where the wafers are coated with copper nanorods layer acting as an adhesive. These two wafers are subsequently subjected to external pressure and temperatures ranging from 200 °C to 400 °C in order to facilitate the formation of nano-structured bond at the copper nanorods/copper nanorods interface.

Figure 2a shows atop view SEM image of as-deposited copper nanorod arrays. Figures 2b-2d show the cross-sectional images of the copper bonding interfaces using FIB/SEM. It is observed that the copper nanorod/copper nanorod interface is partially bonded under the bonding temperature of 200 °C; however original copper rod morphology (in Fig. 2a) has disappeared. Instead, the copper rods fuse together forming a dense structure containing large grains distributing along the film thickness. These grains tend to grow isotropically, suggesting that the grain boundary migrates evenly in all directions associated with the uniform grain boundary energy under isothermal condition. It is observed that the copper grains grow over the copper nanorods/blanket copper film and copper nanorods/copper nanorods interfaces subjected to bonding process. This phenomenon becomes apparent upon bonding temperature ≥ 300 °C, indicating the higher mobility of copper species subjected to elevated temperatures and high pressure.

It is seen that the grain structures of the bonding layers in Figs. 2b-2d contain pores in the grain interior where the interior pores only appear in the region of original copper nanorod layer, in contrast to the original copper blanket layer. Both the number and size of the pores that are present in the bonding structure decrease with increasing the bonding temperatures. Similarly,

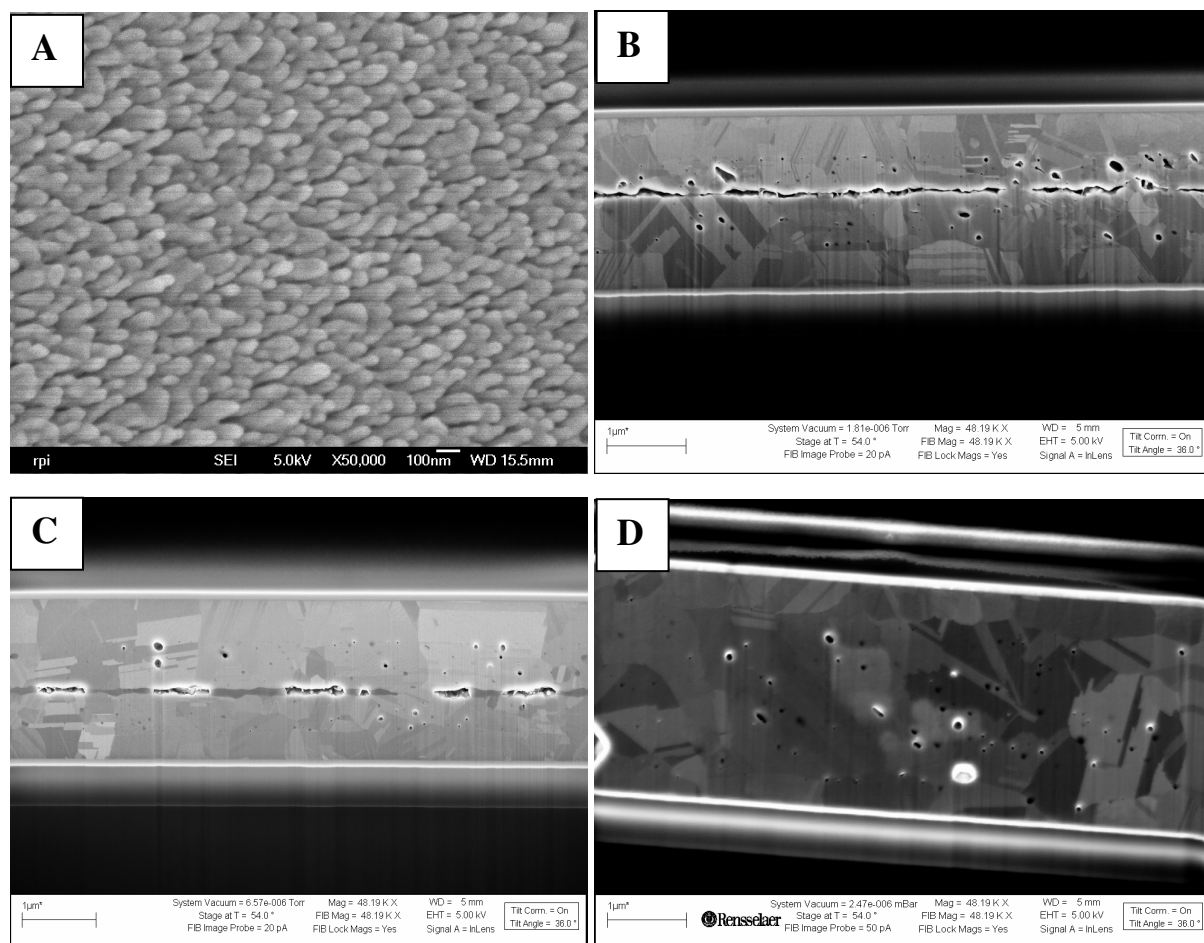


Figure 2 (a) SEM image of as-deposited copper nanorod arrays and cross-sectional FIB/SEM images of copper nanorod bonding at (b) 200 °C, (c) 300 °C, and (d) 400 °C, respectively.

the evolution of the bonding structure in Figs. 2b- 2d clearly shows that the gap appearing at the copper nanorod/copper nanorod interface is diminished as the bonding temperature increases because the mass transport of the copper is more efficient upon higher temperatures. These copper rod bonding characteristics can be realized through the understanding of sintering phenomenon. Sintering is a phenomenon that the metal powders bond together when heated to temperatures in excess of approximately half of the absolute melting temperature. The primary mechanism that drives the sintering process is the reduction of the surface area where the energetic gain comes from the fact that the energy excess of the surface area associates with the metal powders before sintering. At a sufficiently high temperature, mass transport through diffusion process becomes significant.⁹ Here, on microscopic scale, at the necks, which are the points of copper nanorod contacts, the motion of an atom into the neck region is favorable since it reduces the net surface energy by reducing the total surface area.

Figure 2 reveals that the phase transformation temperature of copper nanorod is substantially lower than its bulk melting point of 1085 °C. The threshold of the temperature to activate atomic transport is known to decrease with the shrinkage of particle size, which is the well-known size-dependent melting temperature depression based on Gibbs-Thompson theory. In contrast to the bulk material, the nano-sized copper rods are characterized by the fact that the

ratio of the number of surface to volume atoms is large. The thermodynamic properties of materials therefore confined to small dimensions due to the strong influence of the surface atoms.⁸

During the bonding process, a capillary force,¹⁰ arising from the curvature formed at the contact between neighbouring copper nanorods subjected to bonding force and temperature, provides a sintering driving force. The capillary force is orientated isotropically and provides a compressive stress normal to the neck section between neighbouring copper nanorods. The presence of the mobile layer initiated by surface diffusion during sintering accelerates mass transport and improves sintering densification owing to the intergrain capillary forces. This capillary force can be converted to an equivalent hydrostatic pressure. The capillary pressure, also known as the sintering stress is strongly sensitive to the nanorod size. It is due to the fact that the sintering stress generated by the capillary force associated with smaller nanorods during constant heating rate can lead to significant densification at a lower temperature, as illustrated in Figs. 2b-2d.

The gap appearing at copper nanorods/copper nanorods interface results from the original surface roughness of the nanorod arrays and the global thickness uniformity of the copper films. With respect to diffusion-controlled shrinkage of the voids in the structure, the larger gap at the interface is more resistant to sintering densification, compared with the space among copper nanorods. Therefore, the capillary force due to the atomic mobility at a given low temperature (200 °C – 300 °C) and bonding pressure (0.32 MPa) is not sufficient to fill out the gap. Higher temperature (400 °C) and/or bonding pressure are needed to further soften the parent material in conjunction with a higher sintering stress for densification of the copper nanorod layer. Alternatively, the reduction of the copper nanorod size provides means to accelerate densification by the enhancement of surface diffusion.

It is noted that the external pressure exhibits a prominent enhancement to the diffusion-controlled mass transport process in the copper nanorod layer, which has fused into a continuous microstructure at a low bonding temperature of 200 °C, as shown in Fig. 2b. On the contrary, in the absence of external pressure, copper nanorod arrays after being annealed at the same temperature exhibit no observable change in morphology, with respect to as-deposited copper nanorod arrays, as shown in the SEM images in Fig. 3. In the bonding procedure for copper

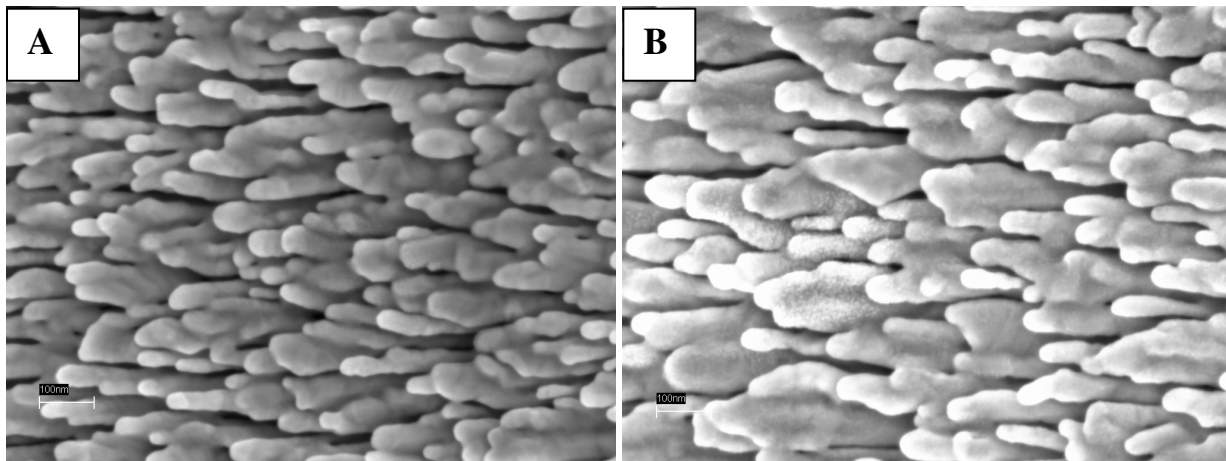


Figure 3 SEM top views of (a) as-deposited copper nanorod arrays and (b) copper nanorods after being annealed at 200 °C for 1 hr.

nanorod layer to achieve consolidation, diffusional creep is a dominating process where the stress directs the diffusional flow. The rate of densification increases with the creep strain rate and the porosity. Under the applied pressure, effective stress is delivered through the contacts among copper rods, leading to the copper nanorod and grain slide and dislocation slip assisted by diffusion process, therefore a more rapid densification is achieved. High levels of porosity contained in the initial copper nanorod layer make the rate of the densification higher because of a higher effective stress where pores act as stress concentrators.

CONCLUSION

In summary, we have discussed the copper wafer bonding by copper nanorod arrays melting at low temperatures. FIB/SEM investigation shows that the copper nanorod arrays have undergone melting process when subjected to bonding temperatures ranging at 200 °C – 400 °C in combination with an external pressure. This low temperature bonding characteristics is realized by understanding the sintering phenomenon. The microstructure evolution shows that the bonding structure is densified with increasing the bonding temperature where the interface is entirely eliminated at bonding temperature of 400 °C. Particularly, the enhancement of fusing behavior for copper nanorod arrays by an external pressure is demonstrated at a low temperature of 200 °C. This is compared to the fact that the copper nanorod arrays alone subjected to annealing at the same temperature exhibits no significant change. Therefore, the morphological change of such nanostructures, which is caused by surface atom mobility, is not only size-dependent, but also influenced by the applied pressure. Our study provides the fact that the copper nanorod arrays are feasible to be used as an adhesive layer for low temperature wafer bonding.

ACKNOWLEDGMENTS

This research program is sponsored by NYSTAR through Focus Center – New York.

REFERENCES

1. J. Voldman, M. L. Gary, and M. A. Schmidt, *Annu. Rev. Biomed. Eng.*, **1**, 401 (1999).
2. F. Niklaus, J.-Q. Lu, G. Stemme, and R. Gutmann, *J. of Appl. Phys. (Applied Physics Review – Focused Review)*, **99** (3), 031101 (2006).
3. A. J. Pitera, G. Taraschi, M. L. Lee, C. W. Leitz, Z.-Y. Cheng, and E. A. Fitzgerald, *Journal of The Electrochemical Society*, **151** (7), G443 (2004).
4. A. Murai, D. B. Thompson, H. Masui, N. Fellows, U. K. Mishra, S. Nakamura, and S. P. DenBaars, *Appl. Phys. Lett.*, **89**, 171116 (2006).
5. J.-Q. Lu, T.S. Cale and R.J. Gutmann, in *Dielectrics for Nanosystems: Materials, Science, Processing, Reliability, and Manufacturing*, ECS PV 2004-04, pp. 312-323 (2004).
6. K. N. Chen, C. S. Tan, A. Fan, and R. Reif, *Electrochemical and Solid-State Letters*, **7** (1), G14 (2004).
7. K.-N. Chen, S.H. Lee, P.S. Andry, C.K. Tsang, A.W. Topol, Y.-M. Lin, J.-Q. Lu, A.M. Young, M. Jeong, and W. Haensch, *2006 IEEE International Electron Devices Meeting (IEDM 2006)*, in press.
8. T. Karabacak, J. S. Deluca, P.-I. Wang, G. A. Ten Eyck, D. Ye, G.-C Wang, and T.-M. Lu. *Journal of Applied Physics*, **99**, 064304 (2006).
9. R. M. German, *Power Metallurgy Science*, Metal Powder Industries Federation, NJ, (1989).
10. J. Liu, A. L. Cardamone, and R. M. German, *Power Metallurgy*, **44** (4), 317 (2001).